Performance Analysis of PLC over Fading Channels with Colored Nakagami-m Background Noise

Yun Ai[1], Tomoaki Ohtsuki[2], and Michael Cheffena[1]
[1]Norwegian University of Science and Technology, N-2815 Gjøvik, Norway; [2]Keio University, 223-8522 Yokohama, Japan
Email: {yun.ai, michael.cheffena}@ntnu.no, ohtsuki@keio.jp

***Abstract*—Power line communication (PLC) is an emerging technology for the realization of smart grid and home automation. It utilizes existing power line infrastructure for data communication in addition to the transmission of power. The PLC channel behaves significantly different from the wireless channel; and it is characterized by signal attenuation as well as by additive noise and multiplicative noise effects. The additive noise consists of background noise and impulsive noise; while the multiplicative noise results in fading of the received signal power. This paper focuses on the impact of the PLC channel characteristics on the outage and BER performance of a PLC system over Rayleigh fading channel with frequency-distance dependent attenuation and colored Nakagami-m distributed additive noise. We derive the exact closed-form expressions for the distribution of the instantaneous signal-to-noise ratio (SNR) and show the detector based the maximum Likelihood (ML) criterion as well as a simple but efficient suboptimal detector. Monte Carlo simulation results are used to verify the derived analytical expressions.**

I. Introduction

In recent years, power line communication (PLC) has gained increasing interests from both the industry and academia due to the vision of widespread information transmission through power lines. With the advantages of omnipresence of power line and no need to invest in new infrastructure, PLC is set to be a promising technology to meet the ever-growing demands of high speed and ubiquitous access to digital information [1]. However, the power line channel presents some constraints for reliable signal transmission such as fading, unpredictable fluctuation of noise levels and impedance, time varying signal attenuation along the transmission line, etc [2].

PLC channel is tremendously different from the wireless channel. Attenuation in PLC systems depends on the characteristics of the power cables, length of transmission, and the operating frequency. The additive noise in PLC can be classified into two broad categories, i.e., background noise and impulsive noise. The impulsive noise is mostly modeled by the Gaussian-mixture distributions, e.g., Bernoulli-Gaussian or Middleton's class-A distributions [2], while studies show that background noise in PLC follows the Nakagami-m distribution [3]–[5]. In addition, the background noise in the PLC channel is not white but colored. In this paper, we focus on the effects of colored background noise due to its different characteristics from the wireless channel. The amplitude fading statistics in PLC environments are not well established compared to wireless communications. A vast number of measurement results show that statistical distributions such as Rayleigh, Rician, and lognormal are recommended for defining the path amplitudes in PLC channels [6]. In our analysis, we will assume that the amplitude follows Rayleigh distribution, which was found to be the best fit for a wealth of PLC field measurements [7]–[11].

Due to the unfavorable characteristics of the PLC channel, performance analysis of PLC systems has been the focus of research. The bit error rate (BER) of a PLC system under the combined effect of background and impulsive noises is analyzed in [12]. The PLC performance in terms of BER and outage probability for a binary phase shift keying (BPSK) modulated signal under Nakagami-m distributed additive noise is studied in [13], where only the noise is taken into account and fading is ignored. The outage performance of PLC channel assuming Rician fading is investigated in [14]. A comparison of BER for an orthogonal frequency division multiplexing (OFDM) system with different pulse-shaping is studied in [15]. The BER and outage performance of PLC using differential BPSK modulation is investigated in [16]. While the the aforementioned works have investigated the PLC performance under different configurations, it is difficult to gain knowledge on the impact of the PLC channel characteristics on the system performance, which will be the focus of this paper.

In this paper, we study the system performance of PLC over Rayleigh fading channel with Nakagami-m distributed additive noise. We derive the expression for the probability density function (PDF) of the instantaneous signal-to-noise ratio (SNR) taking into account the effects of frequency-distance dependent attenuation, Rayleigh fading, and Nakagami-m like additive noise. Based on the above statistics, we investigate impact of the channel characteristics on the outage probability and BER performance.

The remainder of the paper is organized as follows. In Section II, we describe the considered system and channel models. The distribution of the instantaneous SNR is analyzed in Section III; and closed-form expression for the outage probability is derived. In Section IV, we investigated the performance of the optimal and an suboptimal detector under the investigated channel. The analytical and simulation results are presented in Section V. Section VI concludes the paper.

II. System and Channel Model

The input/output model of a PLC system over Rayleigh fading channel with Nakagami-m noise can be expressed as

$$y_c = h_c \cdot x + w_c, \tag{1}$$

where x is the channel input with unit energy, i.e., $\mathrm{E}[|x|^2]=1$; and y_c is the channel output. The envelope h of the complex channel gain h_c is Rayleigh distributed with PDF given by

$$f_h(h)=\frac{h}{\sigma^2}\cdot\exp\Big(-\frac{h^2}{2\sigma^2}\Big), \tag{2}$$

where σ is the scale parameter of the distribution, which determines the statistical average and the variance of the random variable (RV) as $\mathrm{E}[h]=\sigma\sqrt{\pi/2}$ and $\mathrm{Var}[h]=(2-0.5\pi)\sigma^2$, respectively. In model (1), the average power of $h_c\cdot x$ depends on the transmit power P_t and the power attenuation $A(D,f)$ over transmission distance D at operating frequency f[1], i.e.,

$$\mathrm{E}[|h_c|^2\cdot|x|^2]=\mathrm{E}[h^2]=P_t\cdot A(D,f). \tag{3}$$

Due to the nature of the cable propagation environment, the PLC attenuation model is significantly different from that of wireless channel and $A(D,f)$ can be expressed as [17]

$$A(D,f)=e^{-2(\alpha_1+\alpha_2\cdot f^k)\cdot D}, \tag{4}$$

where α_1 and α_2 are constants with dependence on the system configurations; the exponent k is the attenuation factor with typical values between 0.5 and 1. It is obvious from (4) that the attenuation increases dramatically with higher frequency and larger transmission distance.

Utilizing (3), (4) and the equality $\mathrm{E}[h^2]=\mathrm{Var}[h]+(\mathrm{E}[h])^2$, the scale parameter σ in (2) can be represented as

$$\sigma=\sqrt{\frac{P_t}{2}}\cdot e^{-(\alpha_1+\alpha_2\cdot f^k)\cdot D}. \tag{5}$$

In (1), the parameter w_c represents the complex background noise. The absolute value w of the RV w_c is Nakagami-m distributed and its PDF is given by

$$f_w(w)=\frac{2m^m}{\Gamma(m)\Omega^m}w^{2m-1}\cdot\exp\Big(-\frac{mw^2}{\Omega}\Big), \tag{6}$$

where m is the shape parameter of the distribution defined as $\mathrm{E}^2[w^2]/\mathrm{Var}[w^2]$ with $\mathrm{E}[\cdot]$ denoting the expectation operator and $\mathrm{Var}[\cdot]$ representing the variance of the random variable, and $\Gamma(\cdot)$ is the Gamma function. The parameter Ω is the average power defined as $\mathrm{E}[w^2]$. The widely used assumption of white noise for wireless channel does not hold for PLC channel. Instead, the background noise is colored and the average power per unit bandwidth, namely, the power spectral density (PSD), can be written as [17]

$$\Omega=\mathrm{E}[w^2]=10^{0.1\cdot(\beta_1+\beta_2\cdot e^{-f/\beta_3})}\qquad[\mathrm{mW/Hz}], \tag{7}$$

where β_1, β_2, and β_3 are some constants.

III. Outage Performance Analysis

The outage probability is an essential performance criterion quantity for communication systems and is defined as the probability that the SNR γ falls below a predefined threshold γ_{th}. Obviously, we need the knowledge on the distribution of the instantaneous SNR to evaluate the outage probability.

[1]The frequency f is in MHz throughout the paper.

The instantaneous SNR γ of the PLC system in (1) is expressed as

$$\gamma=\frac{h^2}{w^2}. \tag{8}$$

For simplicity of notation, we replace the arguments h^2 and w^2 in (8) by h' and w', respectively. To obtain the statistics of the instantaneous SNR γ, we first need the statistics of $h'=h^2$ and $w'=w^2$. With the RV h following the Raleigh distribution, the RV h' will be distributed according to an exponential distribution given by

$$f_{h'}(h')=f_h(\sqrt{h'})\cdot\Big|\frac{dh}{dh'}\Big|=\frac{1}{2\sigma^2}\cdot\exp\Big(-\frac{h'}{2\sigma^2}\Big). \tag{9}$$

Similarly, the Nakagami-m distributed RV w leads to the RV w' following a gamma distribution with the following PDF:

$$f_{w'}(w')=\frac{m^m}{\Gamma(m)\Omega^m}w'^{(m-1)}\cdot\exp\Big(-\frac{mw'}{\Omega}\Big). \tag{10}$$

After obtaining the PDFs of the RVs h' and w', the PDF of a new RV defined as the quotient of the two RVs $\gamma=\frac{h'}{w'}$ can be obtained as

$$f_\gamma(\gamma)=\int_{-\infty}^{\infty}|w'|\cdot f_{h',w'}(w'\gamma,w')\,dw', \tag{11}$$

where $f_{h',w'}(\cdot,\cdot)$ is the joint PDF of the independent RVs h' and w'. Therefore, $f_{h',w'}(w'\gamma,w')=f_{h'}(w'\gamma)\cdot f_{w'}(w')$. Substituting this equality into (11) and after some manipulations, we obtain the distribution of the instantaneous SNR as

$$\begin{aligned}f_\gamma(\gamma)&=\int_0^\infty w'\cdot f_{h'}(w'\gamma)\cdot f_{w'}(w')\,dw'\\&=\frac{m^m}{2\sigma^2\Omega^m\Gamma(m)}\int_0^\infty w'^m\cdot\exp\Big[-\Big(\frac{\gamma}{2\sigma^2}+\frac{m}{\Omega}\Big)\cdot w'\Big]\,dw'\\&=\frac{m^m}{2\sigma^2\Omega^m\cdot\mathrm{B}(1,m)}\cdot\Big(\frac{\gamma}{2\sigma^2}+\frac{m}{\Omega}\Big)^{-(m+1)},\end{aligned} \tag{12}$$

where $\mathrm{B}(\cdot,\cdot)$ is the Beta function [18, p. 258]; and the last equality is obtained by using [19, Eq. 3.478.1] and the functional relation between Beta function $\mathrm{B}(\cdot,\cdot)$ and Gamma function $\Gamma(\cdot)$ [19, Eq. 8.384].

The cumulative distribution function (CDF) $F_\gamma(\gamma)$ of the RV γ can be immediately obtained from its relationship with the PDF $f_\gamma(\cdot)$, i.e., $F_\gamma(\gamma)=\int_0^\gamma f_\gamma(x)\,dx$, as follows:

$$F_\gamma(\gamma)=\frac{m^m}{2\sigma^2\Omega^m\mathrm{B}(1,m)}\cdot\int_0^\gamma\Big(\frac{x}{2\sigma^2}+\frac{m}{\Omega}\Big)^{-(m+1)}\,dx. \tag{13}$$

In (13), substituting $t=\frac{x}{\gamma}$ and with the appropriate change of the integration limits, the CDF $F_\gamma(\gamma)$ can be rewritten as

$$\begin{aligned}F_\gamma(\gamma)&=\frac{\Omega\gamma}{2\sigma^2m\cdot\mathrm{B}(1,m)}\cdot\int_0^1\Big(1+\frac{\Omega\gamma}{2\sigma^2m}t\Big)^{-(m+1)}\,dt\\&=\frac{\Omega\gamma}{2\sigma^2m\cdot\mathrm{B}(1,m)}\cdot{}_2F_1(m+1,1;2;-\frac{\Omega\gamma}{2\sigma^2m}),\end{aligned} \tag{14}$$

where the last equality comes from the integral representation of Gauss hypergeometric function ${}_2F_1(\cdot,\cdot;\cdot;\cdot)$ [19, Eq. 9.111]. The Gauss hypergeometric function can be straightforwardly evaluated using mathematical softwares such as Matlab and

Mathematica. Then, the outage probability $P_{out} = F_\gamma(\gamma_{th})$ is simply expressed as

$$P_{out}(\gamma_{th}) = \frac{\Omega\gamma_{th}}{2\sigma^2 m \cdot \mathrm{B}(1,m)} \cdot {}_2F_1\Big(m+1, 1; 2; -\frac{\Omega\gamma_{th}}{2\sigma^2 m}\Big). \tag{15}$$

Substituting (5) and (7) into (15), we can further express the outage probability in terms of the parameters related to the PLC attenuation, fading, and additive noise introduced in Section II.

IV. Bit Error Rate Performance Analysis

In this section, we study the BER performance of the PLC system for BPSK signaling under the effects of Rayleigh fading and Nakagami-m background noise.

A. System Model for BER Analysis

Since the BER of the BPSK signals is equal to the BER of the real part (or imaginary part) of the received signals given in (1), we just need to study the real part (or imaginary part) of the signals. The real part $y_r = \mathrm{Re}[y]$ of the received signal y in (1) is expressed by

$$y_r = h_r \cdot s + w_r, \tag{16}$$

where the BPSK symbols $s \in \{\pm 1\}$ are equiprobably modulated and transmitted. It is known that the envelope of a complex Gaussian variable is Rayleigh distributed. Hence, the variable $h_r = \mathrm{Re}[h_c]$ is Gaussian distributed with PDF given by

$$f_{h_r}(h_r) = \frac{1}{\sqrt{2\pi}\sigma} \cdot \exp\Big(-\frac{h_r^2}{2\sigma^2}\Big), \tag{17}$$

where the standard deviation σ of the Gaussian RV has been introduced in (2) and also extended in (5).

The variable w_r in (16) is related to the Nakagami-m RV w in (6) as follows: $w_r = \mathrm{Re}[w_c] = \mathrm{Re}[w \cdot e^{j\theta}] = w \cdot \cos\theta$, where θ is the phase of the noise and is uniformly distributed over $[-\pi, \pi]$. Then the distribution of the RV w_r conditioned on θ can be simply obtained from its above relationship with the RV w and the PDF $f_w(\cdot)$ in (6), which is expressed as

$$\begin{aligned} f_{w_r|\theta}(w_r) &= f_w\Big(\frac{w_r}{\cos\theta}\Big)\Big|\frac{dw}{dw_r}\Big| = \frac{1}{\sqrt{(\cos\theta)^2}} \cdot f_w\Big(\frac{w_r}{\cos\theta}\Big) \\ &= \frac{2w_r^{2m-1} \cdot m^m}{\Gamma(m) \cdot \Omega^m (\cos\theta)^{2m}} \cdot \exp\Big(-\frac{m w_c^2}{\Omega(\cos\theta)^2}\Big), \end{aligned} \tag{18}$$

where the RVs m and Ω have been introduced in (6) and the RV Ω is also extended in (7).

B. The Optimal and Suboptimal Detectors

Using some channel estimation technique, an estimate $\widetilde{h}_r$ of the channel gain is produced. In our analysis, we assume a perfect channel estimation, i.e., $\widetilde{h}_r = h_r$. The observation y_r in (16) is divided by the channel estimate, which results in

$$d = \frac{y_r}{\widetilde{h}_r} = s + \frac{w_r}{h_r} = s + \hat{w}, \tag{19}$$

where $\hat{w} = \frac{w_r}{h_r}$ for the sake of notational simplicity.

Utilizing (17), (18) and the independence between the RVs w_r and h_r, the PDF $f_{\hat{w}|\theta}(\hat{w})$ of the RV $\hat{w}$ conditioned on θ can be expressed after some manipulations as

$$\begin{aligned} f_{\hat{w}|\theta}(\hat{w}) &= \int_{-\infty}^{\infty} |h_r| \cdot f_{w_r|\theta}(\hat{w}h_r) \cdot f_{h_r}(h_r)\, dh_r \\ &= \frac{1}{\sqrt{2\pi}\sigma} \cdot \frac{4\hat{w}^{2m-1}}{\Gamma(m)} \cdot \Big(\frac{m}{\Omega(\cos\theta)^2}\Big)^m \\ &\quad \cdot \int_0^{\infty} h_r^{2m} \exp\Big(-h_r^2\Big(\frac{m\hat{w}^2}{\Omega(\cos\theta)^2} + \frac{1}{2\sigma^2}\Big)\Big)\, dh_r \\ &= \frac{\sqrt{2} \cdot \Gamma(0.5) \cdot (\cos\theta)^{-2m} \cdot m^m \cdot \hat{w}^{2m-1}}{\sqrt{\pi}\sigma \mathrm{B}(0.5, m) \cdot \Omega^m \cdot \big(\frac{m\hat{w}^2}{\Omega(\cos\theta)^2} + \frac{1}{2\sigma^2}\big)^{m+0.5}}. \end{aligned} \tag{20}$$

Integrating the conditional PDF $f_{\hat{w}|\theta}(\hat{w})$ over the statistics of the phase θ, we obtain the closed-form expression for the PDF $f_{\hat{w}}(\hat{w})$ of the RV $\hat{w}$ from Appendix A shown in (21) at the bottom of this page. Substituting (5) and (7) into (21), we obtain the PDF $f_{\hat{w}}(\hat{w})$ in terms of the parameters associated with the PLC attenuation, fading, and additive noise.

The optimal detector based on the maximum likelihood (ML) criterion, which is only the function of the decision parameter $\hat{w}$, can be mathematically expressed as

$$\Pr(d|s=1) \underset{-1}{\overset{1}{\gtrless}} \Pr(d|s=-1). \tag{22}$$

The ML detector in (22) can be reformulated, after some straightforward mathematical manipulations, as

$$g(\hat{w} = d-1) \underset{-1}{\overset{1}{\gtrless}} g(\hat{w} = d+1), \tag{23}$$

where the function $g(\cdot)$ is given in (21).

While the detector in (23) is optimal in terms of BER performance, it is extremely complex and requires a lot of computation. A suboptimal detector used in [3] and [20] is given by

$$d \underset{-1}{\overset{1}{\gtrless}} 0. \tag{24}$$

$$\begin{aligned} f_{\hat{w}}(\hat{w}) &= \int_{-\pi}^{\pi} f_{\hat{w}|\theta}(\hat{w}) \cdot f_\theta(\theta)\, d\theta = \int_{-\pi}^{\pi} \frac{1}{2\pi} \cdot f_{\hat{w}|\theta}(\hat{w})\, d\theta \\ &= \frac{2\sqrt{2\Omega} \cdot \Gamma(m+0.5)}{\pi\sigma\sqrt{\pi m} \cdot \Gamma(m)} \cdot \underbrace{\Bigg[\frac{{}_3F_2\big(1, \frac{1}{2}, \frac{1}{2}+m; \frac{3}{2}, \frac{3}{2}; -\frac{\Omega}{2m\sigma^2\hat{w}^2}\big)}{\hat{w}^2} - \frac{(2m+1)\cdot\Omega}{9m\sigma^2\hat{w}^4} \cdot {}_3F_2\Big(2, \frac{3}{2}, \frac{3}{2}+m; \frac{5}{2}, \frac{5}{2}; -\frac{\Omega}{2m\sigma^2\hat{w}^2}\Big)\Bigg]}_{g(\hat{w})}. \end{aligned} \tag{21}$$

Despite that the threshold-based detector in (24) is not optimal for communication systems over fading channels with Nakagami-m additive noise, it is much simpler and more practical for time critical missions. For a rough comparison, the elapsed time for the optimal ML based detector is around 1.07 seconds when running the program with Matlab R2015b 8.6.0.267246 on a Microsoft Windows® machine with Intel(R) Core(TM) i7-3740QM 2.70GHz CPU; while the elapsed time is less than 0.008 seconds for the suboptimal detector running with the same configuration. In addition, the suboptimal detector also suffices for our analysis on the impact of various PLC channel characteristics on the PLC system performance, which were not covered in other related works.

With the suboptimal detector in (24), the average BER of the binary transmitted symbols over Rayleigh fading with Nakagami-m distributed additive noise can be written as

$$P_e = \int_1^{\infty} f_{\hat{w}}(\hat{w})\, d\hat{w}, \tag{25}$$

where $f_{\hat{w}}(\hat{w})$ is given in (21). It is not possible to obtain closed-form expressions for the integral in (25), but it is simple and straightforward to evaluate it numerically using mathematical softwares such as Matlab and Mathematica.

C. Optimal Transmission Frequency

Different from its wireless counterpart, the transmission frequency of the PLC system influences both the attenuation and the noise that the system will experience. It is intuitive to see that with the same fading and noise distributions, the channel with the highest average SNR will outperform. Then, we start with the average SNR $\overline{\gamma}$ of the channel given by

$$\overline{\gamma} = \frac{\mathrm{E}[h^2]}{\mathrm{E}[w^2]} = \frac{P_t \cdot e^{-2(\alpha_1+\alpha_2 \cdot f^k)\cdot D}}{10^{0.1\cdot(\beta_1+\beta_2\cdot e^{-f/\beta_3})}}. \tag{26}$$

Then, the optimal frequency f_{opt} in terms of BER and outage probability can be obtained with the gradient descent method, i.e., taking the first derivative of the strictly monotonic increasing function $\log_{10}(\overline{\gamma})$ with respect to f and setting the derivative to 0:

$$\frac{d}{df}\left[-2D\cdot(\alpha_1+\alpha_2\cdot f^k)\cdot\log_{10} e - 0.1\cdot(\beta_1+\beta_2\cdot e^{-f/\beta_3})\right]$$
$$= -2\alpha_2 kD(\log_{10} e) f^{k-1} + \frac{0.1\beta_2}{\beta_3} e^{-f/\beta_3} = 0. \tag{27}$$

The solution to the above equation in (27) cannot be expressed with elementary functions and a solution of the equation in terms of Lambert W function is derived from Appendix B as follows:

$$f_{opt} = (k-1)\beta_3 \cdot W\left(\frac{\left(20(\log_{10} e)\alpha_2 kD\cdot\beta_3^k\right)^{\frac{1}{1-k}}}{(k-1)\cdot\beta_2^{\frac{1}{1-k}}}\right), \tag{28}$$

where $W(\cdot)$ is the Lambert W function (a.k.a., Omega function), which is defined as the multi-valued inverse of the function $x \mapsto xe^x$ [21]. It can be effectively evaluated using the Matlab function $lambertw(\cdot,\cdot)$. Obviously, the optimal carrier frequency is a function of the transmission distance D, which is quite different from that of wireless communications.

TABLE I: Simulation Parameters

attenuation model parameters		
$\alpha_1 = 9.33\times10^{-3}$ m^{-1}	$\alpha_2 = 5.1\times10^{-3}$ s/m	$k = 0.7$
noise model parameters (residential environment)		
$\beta_1 = -125$	$\beta_2 = 35$	$\beta_3 = 3.6$
noise model parameters (industrial environment)		
$\beta_1 = -123$	$\beta_2 = 40$	$\beta_3 = 8.6$
Nakagami-m parameter: $m = 0.8$		

V. Numerical Results

In this section, the analytical expressions presented in the previous sections are evaluated numerically and validated using simulations. We adopt the PLC channel parameter values shown in Table I, which are the experimental data from field measurements conducted in residential and industrial environments [22], [23].

Figure 1 displays the outage probability for different frequencies and threshold SNR in the measured residential and industrial environments. It can be seen that the outage probabilities at different frequencies are significantly different. Given the same propagation environment, the outage probability is greater for higher values of threshold SNRs, which is in accordance with the fact that the outage probability is the CDF of instantaneous SNR. Meanwhile, the outage performance in the measured industrial environment is much worse than that in the measured residential environment. This is due to stronger disturbance by large electrical loads in the industrial scenario, which leads to higher background noise level compared to that in the residential environment.

The average BER performance versus input power under different propagation conditions is shown in Fig. 2. A high dependency of the BER on the transmission frequency can be observed from the results. The BER also increases significantly with longer transmission distance. When the Nakagami-m parameter increases, the BER performance degrades slightly.

Figure 3 compares the BER performance under the electromagnetic compatibility (EMC) regulations in three different regions, i.e., the Federal Communications Commission (FCC) Part 15 from the United States, German Law NB30, and

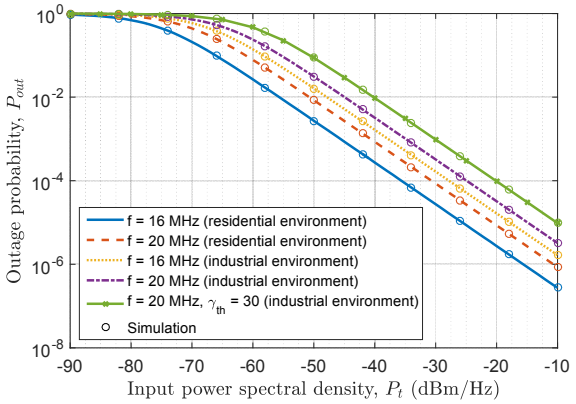

Fig. 1: Outage probability v.s. input power per unit bandwidth with different frequencies, $\gamma_{th} = 10$ unless stated otherwise, $D = 100$ m.

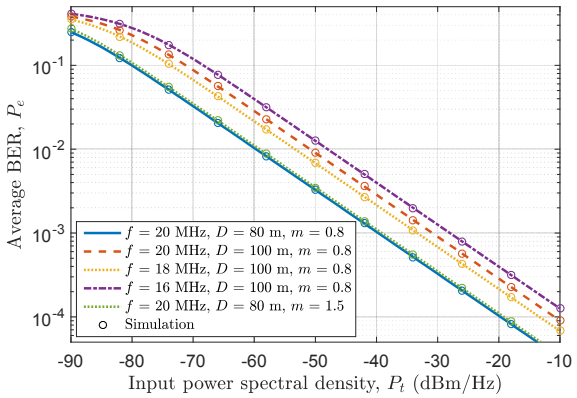

Fig. 2: Average BER v.s. input power per unit bandwidth with different transmission lengths and frequencies in residential environment.

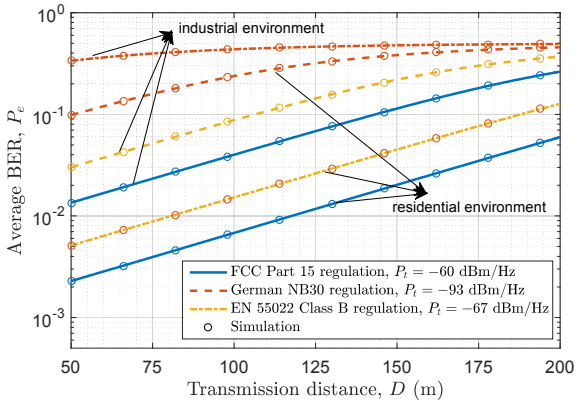

Fig. 3: Average BER v.s. distance in the industrial and residential environments under three different EMC regulations, $f = 3.6$ MHz.

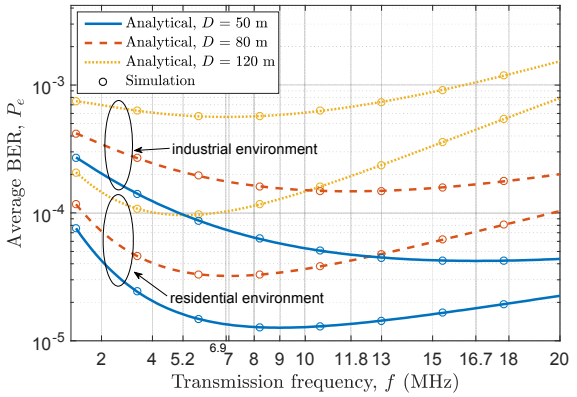

Fig. 4: Average BER v.s. transmission frequency with different transmission lengths, the input PSD is -20 dBm/Hz.

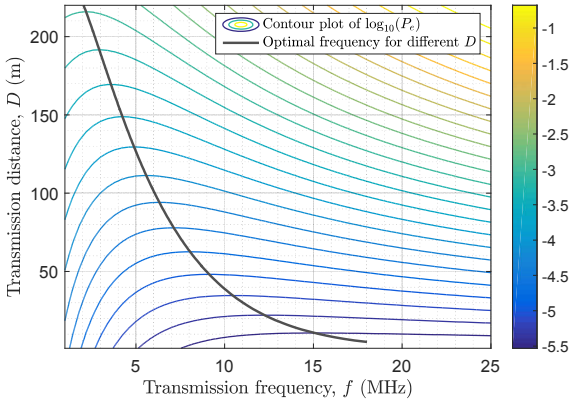

Fig. 5: Contour plot of $\log_{10}(P_e)$ for different transmission frequency and distance in the measured residential environment.

EN55022 Class B from the European Union [17]. EMC regulations in different regions pose different requirements on transmit power. These differences from the regulations clearly result in different achievable performance in different regions.

Figure 4 illustrates the average BER against carrier frequency with different transmission lengths in the measured residential and industrial environments. For a given wireless channel with fixed transmit power and propagation distance, larger carrier frequency generally indicates worse BER performance due to higher attenuation. This is only partially true for the power line channel due to its different characteristics of the background noise. For a PLC link, the BER first decreases with larger carrier frequency before reaching the optimal frequency, then it increases with increasing frequency. Also, this optimal transmission frequency is lower for longer transmission distance. This monotone decreasing trend can also be seen from Fig. 5, which illustrates the relationship between the PLC transmission distance and the corresponding optimal carrier frequency in terms of BER. By comparing the longest transmission distance in the contour plot and the optimal frequency curve in Fig. 5, the validity of the expression (28) is verified.

VI. Conclusion

In this paper, we studied the impact of PLC channel characteristics on the PLC system performance. The effects of the channel characteristics including frequency-distance dependent attenuation, Rayleigh fading, and colored Nakagami-m like additive noise, on the outage and BER performance of the PLC system were evaluated. Exact closed-form expressions for the SNR and expressions for the average BER were derived. The analytical expressions were validated using Monte Carlo simulation results.

Appendix A
Derivation of the PDF $f_{\hat{w}}(\hat{w})$ of the RV $\hat{w}$ in (21)

It is not quite straightforward to solve the integral $f_{\hat{w}}(\hat{w}) = \int_{-\pi}^{\pi} \frac{1}{2\pi} \cdot f_{\hat{w}|\theta}(\hat{w})\, d\theta$ directly. Thus, we first make a change of RV $z = \hat{w}^2$ and solving for $f_z(z)$ by differentiating its CDF $F_z(z)$, then we obtain the desired expression with a change of RV again.

Using the same rationale as in (9), the PDF $f_{z|\theta}(z)$ of the RV $z = \hat{w}^2$ conditioned on θ is expressed as

$$f_{z|\theta}(z) = \frac{\Gamma(m+0.5) \cdot m^m z^{m+1}}{\sqrt{2\pi}\sigma\Omega^m(\cos\theta)^{2m} \cdot \Gamma(m) \cdot \left(\frac{mz}{\Omega(\cos\theta)^2} + \frac{1}{2\sigma^2}\right)^{m+0.5}}. \tag{29}$$

From (29), the CDF $F_{z|\theta}(z)$ of z conditioned on θ, i.e., $F_{z|\theta}(z) = \int_0^z f_{z|\theta}(x)\, dx$, can be written as

$$F_{z|\theta}(z) = \frac{\Gamma(m+0.5)m^m}{\sqrt{2\pi}\sigma\Omega^m(\cos\theta)^{2m}\Gamma(m)} \cdot \int_0^z \frac{x^{m+1}\, dx}{\left(\frac{mx}{\Omega(\cos\theta)^2} + \frac{1}{2\sigma^2}\right)^{m+0.5}}. \tag{30}$$

Substituting $\frac{x}{z} = t$ in the integral in (30) and utilizing the equality [19, Eq. 9.111], we obtain, after some mathematical manipulations, the closed-form expression for the CDF $F_{z|\theta}(z)$ as follows

$$F_{z|\theta}(z) = 1 - \frac{\sqrt{2\Omega}|\cos\theta| \cdot \Gamma(0.5)}{\sigma\sqrt{\pi m z} \cdot \mathrm{B}(0.5, m)} {}_2F_1\Big(\frac{1}{2}, \frac{1}{2}+m; \frac{3}{2}; \frac{\Omega(\cos\theta)^2}{-2m\sigma^2 z}\Big). \quad (31)$$

Integrating the conditional CDF $F_{z|\theta}(z)$ over the statistics of θ, the CDF $F_z(z)$ can be expressed as

$$\begin{aligned} F_z(z) &= \frac{1}{2\pi} \cdot \int_{-\pi}^{\pi} F_{z|\theta}(z)\, d\theta = 1 - \frac{\sqrt{2\Omega} \cdot \Gamma(0.5)}{2\pi\sigma\sqrt{\pi m z} \cdot \mathrm{B}(0.5, m)} \\ &\quad \cdot \int_{-\pi}^{\pi} \sqrt{(\cos\theta)^2} \cdot {}_2F_1\Big(\frac{1}{2}, \frac{1}{2}+m; \frac{3}{2}; -\frac{\Omega(\cos\theta)^2}{2m\sigma^2 z}\Big)\, d\theta \\ &= 1 - \frac{2\sqrt{2\Omega}\Gamma(m+0.5)}{\pi\sigma\sqrt{\pi m z} \cdot \Gamma(m)} {}_3F_2\Big(1, \frac{1}{2}, \frac{1}{2}+m; \frac{3}{2}, \frac{3}{2}; \frac{-\Omega}{2m\sigma^2 z}\Big), \end{aligned} \quad (32)$$

where the last equality is based on the serial representation of the generalized hypergeometric function [19, Eq. 9.14.1] and the equality [19, Eq. 3.621.4].

Next, we can obtain the PDF $f_z(z)$ by differentiating $F_z(z)$ as follows

$$\begin{aligned} f_z(z) = \frac{\sqrt{2\Omega} \cdot \Gamma(m+0.5)}{\pi\sigma\sqrt{\pi m} \cdot \Gamma(m)} \cdot \Bigg[& \frac{{}_3F_2\big(1, \frac{1}{2}, \frac{1}{2}+m; \frac{3}{2}, \frac{3}{2}; -\frac{\Omega}{2m\sigma^2 z}\big)}{z^{1.5}} \\ & - \frac{(1+2m)\Omega}{9m\sigma^2 z^{2.5}} \cdot {}_3F_2\Big(2, \frac{3}{2}, \frac{3}{2}+m; \frac{5}{2}, \frac{5}{2}; \frac{-\Omega}{2m\sigma^2 z}\Big)\Bigg], \end{aligned} \quad (33)$$

where, to obtain (33), we have used the property of the differentiation of generalized hypergeometric functions [24, Eq. (07.27.20.0013.01)] and the chain rule for differentiating composite functions [25, pp. 106–107].

Finally, utilizing the functional relationship between the PDFs $f_{\hat{w}}(\cdot)$ and $f_z(\cdot)$, i.e., $f_{\hat{w}}(\hat{w}) = 2|\hat{w}| \cdot f_z(\hat{w}^2)$, we can obtain the expression for the PDF $f_{\hat{w}}(\hat{w})$ as shown in (21).

Appendix B
Derivation of the optimal frequency in (28)

The relation (27) can be simplified as $x^a e^{-x} = b$ with following change of RVs:

$$a = 1-k, \;\; b = \big(20(\log_{10} e)\alpha_2 k D \beta_3^k\big)/\beta_2, \;\; x = f/\beta_3. \quad (34)$$

Therefore, to obtain the optimal frequency $f_{opt} = \beta_3 x$, we just need to work out the solution of $x^a e^{-x} = b$.

According to the definition of Lambert W function, the solution of the equation $ye^y = X$ is given by $y = W(X)$, where $W(\cdot)$ is the Lambert W function. Substituting y and X with $-\frac{x}{a}$ and $-\frac{b^{\frac{1}{a}}}{a}$, respectively and with some manipulations, the solution of $x^a e^{-x} = b$ can be written as

$$x = -a \cdot W\big(-b^{\frac{1}{a}}/a\big). \quad (35)$$

Substituting a, b, and x back into (35), we can obtain the result shown in (28).

Acknowledgment

We gratefully acknowledge the Regional Research Fund of Norway (RFF) for supporting our research.

References

[1] S. Galli, A. Scaglione *et al.*, "For the grid and through the grid: The role of power line communications in the smart grid," *Proc. IEEE*, vol. 99, no. 6, pp. 998–1027, May 2011.

[2] N. Pavlidou, A. H. Vinck *et al.*, "Power line communications: State of the art and future trends," *IEEE Commun. Mag.*, vol. 41, no. 4, pp. 34–40, Apr. 2003.

[3] H. Meng, Y. L. Guan *et al.*, "Modeling and analysis of noise effects on broadband power-line communications," *IEEE Trans. Power Del.*, vol. 20, no. 2, pp. 630–637, Apr. 2005.

[4] X. Yang, T. Zheng *et al.*, "Investigation of transmission properties on 10-kV medium voltage power lines–part I: General properties," *IEEE Trans. Power Del.*, vol. 22, no. 3, pp. 1446–1454, July 2007.

[5] Y. Kim, S. Choi *et al.*, "Closed-form expression of Nakagami-like background noise in power-line channel," *IEEE Trans. Power Del.*, vol. 23, no. 3, pp. 1410–1412, Apr. 2008.

[6] S. Güzelgöz, H. Arslan *et al.*, "A review of wireless and PLC propagation channel characteristics for smart grid environments," *J. Electr. Comput. Eng.*, vol. 2011, pp. 1–12, Aug. 2011.

[7] P. Karols, K. Dostert *et al.*, "Mass transit power traction networks as communication channels," *IEEE J. Sel. Areas Commum.*, vol. 24, pp. 1339–1350, July 2006.

[8] S.-C. Kim, J.-H. Lee *et al.*, "Wideband channel measurements and modeling for in-house power line communication," in *Proc. of Int. Symp. Power Line Commun. and its Applic. (ISPLC)*, 2002.

[9] M. Tlich, A. Zeddam *et al.*, "Indoor power-line communications channel characterization up to 100 MHz–part I: One-parameter deterministic model," *IEEE Trans. Power Del.*, vol. 23, no. 3, pp. 1392–1401, June 2008.

[10] K. Hoque, L. Debiasi *et al.*, "Performance analysis of MC-CDMA power line communication system," in *Proc. of Int. Conf. Wireless and Opt. Commun. Netw. (WOCN)*. IEEE, 2007, pp. 1–5.

[11] P. Karols, *Nachrichtentechnische Modellierung von Fahrleitungsnetzen in der Bahntechnik*. Mensch-und-Buch-Verlag, 2004.

[12] A. Mathur, M. R. Bhatnagar *et al.*, "Performance evaluation of PLC under the combined effect of background and impulsive noises," *IEEE Commun. Lett.*, vol. 19, no. 7, pp. 1117–1120, May 2015.

[13] A. Mathur and M. R. Bhatnagar, "PLC performance analysis assuming BPSK modulation over Nakagami-m additive noise," *IEEE Commun. Lett.*, vol. 18, no. 6, pp. 909–912, Apr. 2014.

[14] A. Mathur, M. R. Bhatnagar *et al.*, "Outage probability analysis of PLC with channel gain under Nakagami-m additive noise," in *IEEE 82nd Veh. Technol. Conf. (VTC Fall)*. IEEE, 2015, pp. 1–7.

[15] J. J. Sánchez-Martínez, J. A. Cortés *et al.*, "Performance analysis of OFDM modulation on indoor PLC channels in the frequency band up to 210 MHz," in *Proc. of Int. Symp. Power Line Commun. and its Applic. (ISPLC)*, 2010.

[16] A. Mathur, M. R. Bhatnagar *et al.*, "On the performance of a PLC system assuming differential binary phase shift keying," *IEEE Commun. Lett.*, vol. 20, no. 4, pp. 668–671, Feb. 2016.

[17] X. Cheng, R. Cao *et al.*, "Relay-aided amplify-and-forward powerline communications," *IEEE Trans. Smart Grid*, vol. 4, no. 1, pp. 265–272, Jan. 2013.

[18] M. Abramowitz and I. A. Stegun, *Handbook of Mathematical Functions: with Formulas, Graphs, and Mathematical Tables*. Courier Corporation, 1964, no. 55.

[19] A. Jeffrey and D. Zwillinger, *Table of Integrals, Series, and Products*, 7th ed. Elsevier, 2007.

[20] Y. Kim, S.-W. Rhee *et al.*, "BER performance of QPSK-transmitted signal for power line communication under Nakagami-like background noise," *J. Int. Council on Elect. Eng.*, vol. 4, no. 1, pp. 54–58, Sept. 2014.

[21] R. M. Corless, G. H. Gonnet *et al.*, "On the Lambert W function," *Advances in Comput. Math.*, vol. 5, no. 1, pp. 329–359, 1996.

[22] M. Zimmermann and K. Dostert, "A multipath model for the powerline channel," *IEEE Trans. Commun.*, vol. 50, no. 4, pp. 553–559, Aug. 2002.

[23] H. Philipps, "Development of a statistical model for powerline communication channels," in *Proc. of Int. Symp. Power Line Commun. and its Applic. (ISPLC)*, 2000, pp. 5–7.

[24] Wolfram Research. The Wolfram Functions Site. [Online]. Available: http://functions.wolfram.com/

[25] T. M. Apostol, *Mathematical Analysis*, 2nd ed. Addison Wesley Publishing, 1974.